Fabrication of Silver doped Buckypaper and Investigation of its Properties

Yoan Zhi* and Silvia Tokomatov

Department of Chemical Engineering, University of Shanghai, China

Abstract

Microwave absorbing property of composites containing Ag nanoparticles filled multiwalled carbon nanotube buckypaper (Ag-BP) has been investigated. Buckypaper doped with silver was prepared by direct dispersion and filtration method. From the low temperature resistivity measurement it was found that increasing doping level decreases the electrical conductivity of the buckypaper. 30 wt. % and 40 wt. % of Ag-BP samples shows the maximum transmission coefficient, with very high conductivity. The results demonstrate that microwave absorption of Ag-BP was attributed only due to the dielectric loss rather than other losses.The absorption peak frequency of the Ag/MWCNTs BP can be controlled easily in the presence of Ag nanoparticles into the CNT mats.

Keywords: Buckypaper, Doping, Microwave, Resistivity, Transmission coefficient

© 2016 Published by Journal of Nanoanalysis.

1. Introduction

Carbon nanotubes are the promising candidate for the ideal microwave absorbing material[1-3], due to their light weight, high corrosion resistance,high electrical and thermal conductivity and exceptionally high mechanical properties. Great advances in the functionalization of carbon nanotubes with metal particles, polymers and semiconductors have been accomplished in the recent decades[4-6]. Especially, the absorption properties of carbon nanotubes in the lower microwave frequency S-band (2-4 GHz) are importantin theory and actual application such as, Wi-Fi network at 2.4 GHz, microwave ovens at 2.45 GHz and fixed satellite at 2.4, 2.6 GHz and both the absorbing peak frequency position and bandwidth are considered of equal importance. As a lightweight microwave absorber, the microwave carbon nanotubes have been considerably researched for their good compatibility and small density. The development of radar-absorbing materials that work in the radar frequency (*i.e.* GHz) had obtained a big momentum due to their potential applications in the stealth technology of aircrafts and microwave dark-room and protection. Radar-absorbing material is expected to absorb the emitted electromagnetic energy and to minimize the wave reflected in the direction of an energy radar receiver. To optimize the performances of carbon nanotubes as a radar-absorbing material, it is necessary to attach or encapsulate functional groups or

* Corresponding author: Tel:+885127482154, Email: y.zhi@ushanghai.edu.cn

other nanostructures to the surfaces or cavities of the carbon nanotubes. In the earlier reports the microwave-absorbing properties of carbon nanotubes can be enhanced by the incorporation of metal particles such as Co, Fe, Ni and metal oxide such as ZnO or La(NO$_3$)$_3$.

Buckypaper is a kind of carbon nanotube film prepared by the filtration of carbon nanotubes on porous membrane. The van der Waals interactions among carbon nanotubes attract them together and arrange into close-packed bundles[15]. Carbon nanotubes inside buckypaper are randomly distributed and arranged into a nonwoven fibrous structure, asordinary paper made from wood pulp fiber. In this work, silver nanoparticle doped MWCNT buckypaper was prepared by the direct dispersion method. The transmission coefficient (S21) of this metal dispersed buckypaper was observed for different doping of percentage silver for the efficient microwave absorption was studied. All the above investigations are related to the frequency range of 1-18 GHz.

2. Material and Instruments

Synthesis of silver nanoparticles: Metallic silver nanoparticles was prepared by thermal evaporation method and were deposited inside the deposition chamber under a relative pressure of 5 × 10^{-5} torr in the Ar gas atmosphere (350 mtorr).

3. Results and Discussions

3.1 Synthesis of tetraphenyl porphyrins

The amount of 20.6 g of 4-chlorobenzaldehyde was taken in the round bottom flask and it was fitted with water condenser. Round bottom flask was placed on the heating mental. The amount of 350 ml of propanoic acid was added in the round bottom flask and refluxed it for 5 to 10 minutes. The temperature of heating mantle was set around 60 centigrade after 10 to 15 minutes, pyrrole was added from the top of the condenser in 10 ml and the reflux time is 20 to 30 minutes [23]. Propanoic acid is separated by vacuum distillation and the compound is washed with methanol and mixture was allowed to cool and the crystals of TPP were filtered through Buckner funnel [24]. The crystal was dried in vacuum desiccators. Purple color compound was obtained and the yield is 13%. Melting point is 350 ^{0}C. The compound name is 5, 10, 15, 20-tetrakis (4'-chlorophynyl) porphyrins (TCPP).
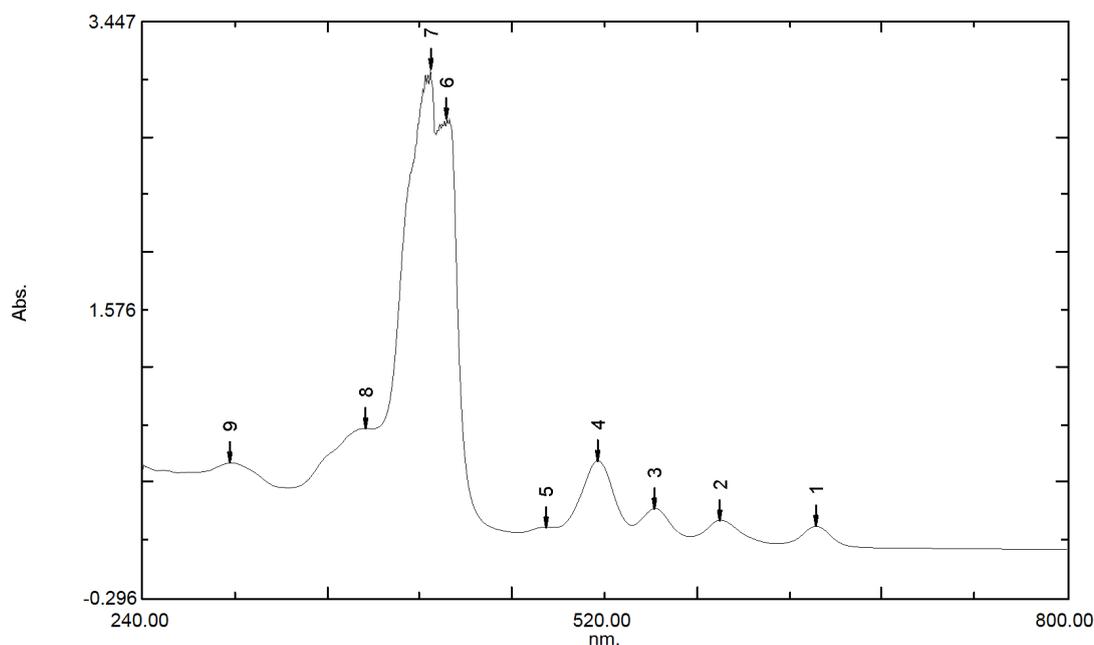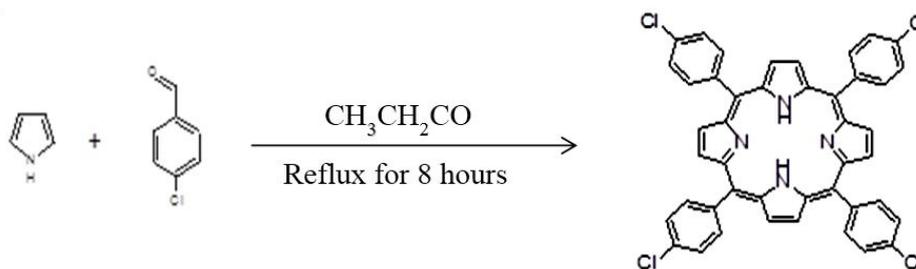

Figure 1. UV-visible spectrum of tetraphenyl porphyrins

Scheme 1. Formation of tetraphenyl porphyrin (M may be Ni, Cu, Co, Fe).

3.2 Purification of tetraphenyl porphyrins

The tetrachlorophenyl porphyrin was developed by Edler [12] and Ruthmend Synthesis [13]. The formation of compound was confirmed by IR method. The main problem in porphyrin separation is the formation of side reaction. In this regard there are so many impurities like propanoic acid derivatives and pyrrole impurities. Purification of crystals can be obtained by using a column. These purpose different solvents were selected along with silica gel. Firstly the column was filled with silica gel along with THF solvent. But the final solvent in column was dichloromethane. Porphyrins elute in a second step [12]. During the formation of porphyrin the reaction can be checked by using TLC. The solvents would be chloroform and n-hexane in 1:3 ratios. The formation of green color in HCl solution confirms the formation of porphyrins.

3.3 Synthesis of tetraphenyl porphyrin metal complex

The synthesis of 5, 10, 15, 20-tetrakis (4-chlorophynyl) porphyrinatometalr (II) was carried out as follows. The amount of 0.5 g of tetrachlorophenyl porphyrin was dissolved in 1.766g of cupric chloride or cupric acetate with the presence of DMF (50 ml) and refluxed it for 5 to 6 hours. These chemicals were taken in the round bottom flasks and a condenser is set on a heating mental. The temperature was set at 60 to 70 ^{0}C. It is the continuation of two pot synthesis. The scheme of complex formation has been discussed in the scheme 1 [12]. The formation of the complex can be confirmed by TLC after every half an hour. The solvent mixture is in the ratio of 1:3 of chloroform and normal hexane. TLC analysis will show the two bands of which one will be of TCPPCu and after the reflux the DMF will remove in half of quantity through vacuum distillation. In the final step the complex will be treated with 6M HCl solution. In this respect 20 ml of 6 M HCl solution will be taken. The complex formed was filtered and TLC analysis confirmed color change in HCl solution.
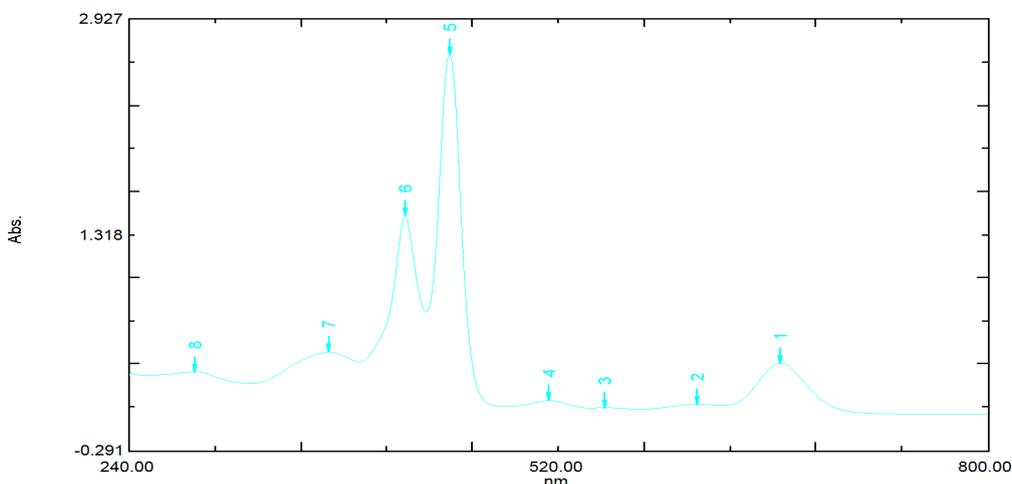

Figure 2. UV-visible spectrum of TCPPFe

Table 1 IR data of the porphyrin and its transition metal complexes

compound	$^1\nu_{N-H}$ cm^{-1}	ν_{C-H} cm^{-1}	$N_{C=C}$ cm^{-1}	ν_{C-N} cm^{-1}	ν_{M-N} cm^{-1}	ν_{M-Cl} cm^{-1}	$^2\nu_{N-H}$ cm^{-1}	$\nu_{(CH2)n}$ cm^{-1}
TCPP	3305.7	2926	1511	1177	---	---	981	730
TCPPFe	---	3024	1395	1232	1012	416	997	723
TCPPCo	---	2780	1634	1350	1014	434	965	715
TCPPNi	---	2780	1626	1350	1014	440	1003	791
TCPPCu	---	2170	1368	1218	980	411	986	702

3.4 IR analysis of tetraphenyl porphyrins

An infrared spectrum of tetra phenyl porphyrin is presented in figure 1 and indicates that at 3305.7 cm^{-1} is the peak because of N-H bond of pyrrole whereas at 2926 cm^{-1} and 2844cm^{-1} is the peak because of C-H bond of pyrrole. It further shows that at 1558 cm^{-1} is the peak due to the C=C of TCPP and 1174 cm^{-1} is the peak due to C-N bond. It is clear from the result that at 981cm^{-1} is another peak of N-H of pyrrole.

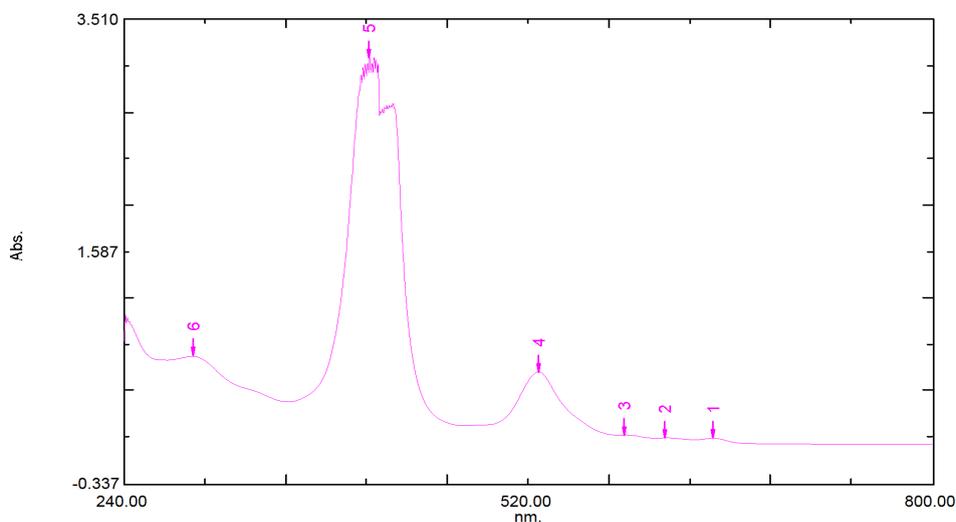## 3.5 IR analysis of tetraphenyl porphyrin nickel complex

The peak for stretching frequency of N-H of pyrrole is absent whereas presence of peak at 2780 cm^{-1} is for (C-H) of pyrrole whereas the C=C and C-N Stretching frequency of benzene and pyrolle respectively explain the formation the complex [13], (CH$_2$)$_n$ peak is at 721 cm^{-1}. For N-H of pyrrole absorption occur at 1014 cm^{-1}.

3.6 IR analysis of tetraphenyl porphyrin iron complex

The peak due to stretching frequency of N-H of pyrrole is absent which is due to the insertion of Fe ion whereas 3024 cm^{-1} is the peak of(C-H) of pyrrole whereas the C=C and C-N stretching frequency of benzene and pyrrole respectively explains the formation the complex, (CH$_2$)n peak is 723 cm^{-1}

3.7 IR analysis of tetraphenyl porphyrin cobalt complex

IR absorption frequencies were different for free base porphyrins and TCPPCo. The absence of stretching frequency of (N-H) bond of free base is due to the coordination of Co metal ion with nitrogen.[37] When cobalt atom is inserted into the free base porphyrins (N-H) bond vibration of free porphyrin is eliminated and the characteristics functional group of Co-N bond is formed and vibrates at 1000 cm^{-1} [14]. This indicates the formation of TCPPCo. The band at 2923-3133 cm^{-1} is due to C-H bond between benzene ring and pyrrole ring.

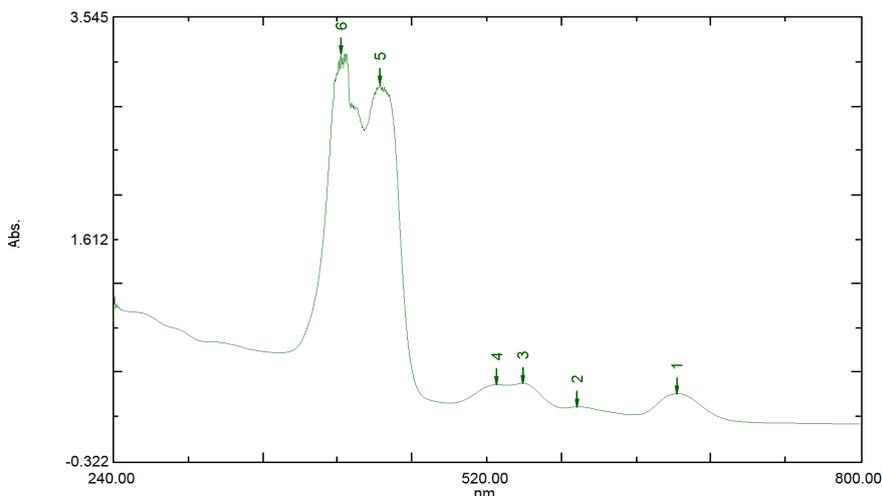**Figure 3.** UV-visible spectrum of TCPPCo.
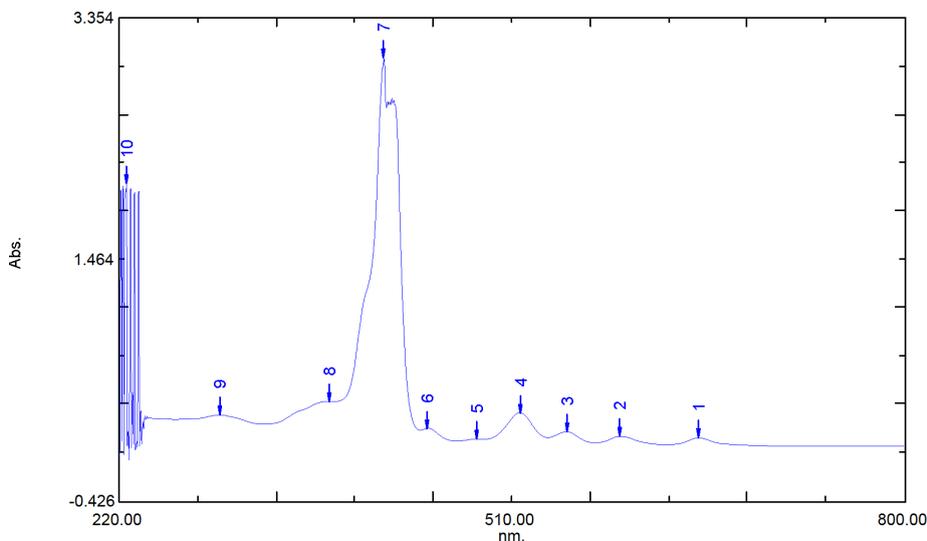
Figure 4. UV-visible spectrum of TCPPNi.

Figure 5. UV-visible spectrum of TCPPCu.

3.8 IR analysis of tetraphenyl porphyrin copper complex

The peak at 2173 cm^{-1} is the peak of pyrrole C-H bond whereas the peak of 1733 cm^{-1} is the peak of C=C shows that the complex has been developed. The peak at 980 cm^{-1} confirms the stretching frequency of (Cu-N), whereas the Peak at 411 cm^{-1} shows the stretching frequency of (Cu-Cl). At 1218 cm^{-1} is the peak of (C-N) of TCCPCu and at 702 cm^{-1} is the peak of $(CH_2)_n$ of pyrrole [14].

3.9 Raman spectroscopic studies

The representative Raman spectra of compounds TCPPFe, TCPPCo and TCPPNi are presented in figure 5. The optical spectra of metalloporphyrins are in general dominated by Q_v to Q^* transitions of the porphyrin core, which provides soret, Q and Q_v features in the absorption spectra [25]. It is based on D_{4h} symmetry. The phenyl ring of porphyrins are exactly perpendicular to the porphyrin plane, the porphyrins has 71 in plane modes [40] while normal spectrum contains 27 in plane vibrations. 9 of 27 are polarized (A_{1g}) and 18 are depolarized (B_{1g}) and (B_{2g}). The infra-red spectrum is maximum 18 modes with E_U symmetry. Porphyrin core has D_{4h} model has 34 out of plane mode of vibrations.
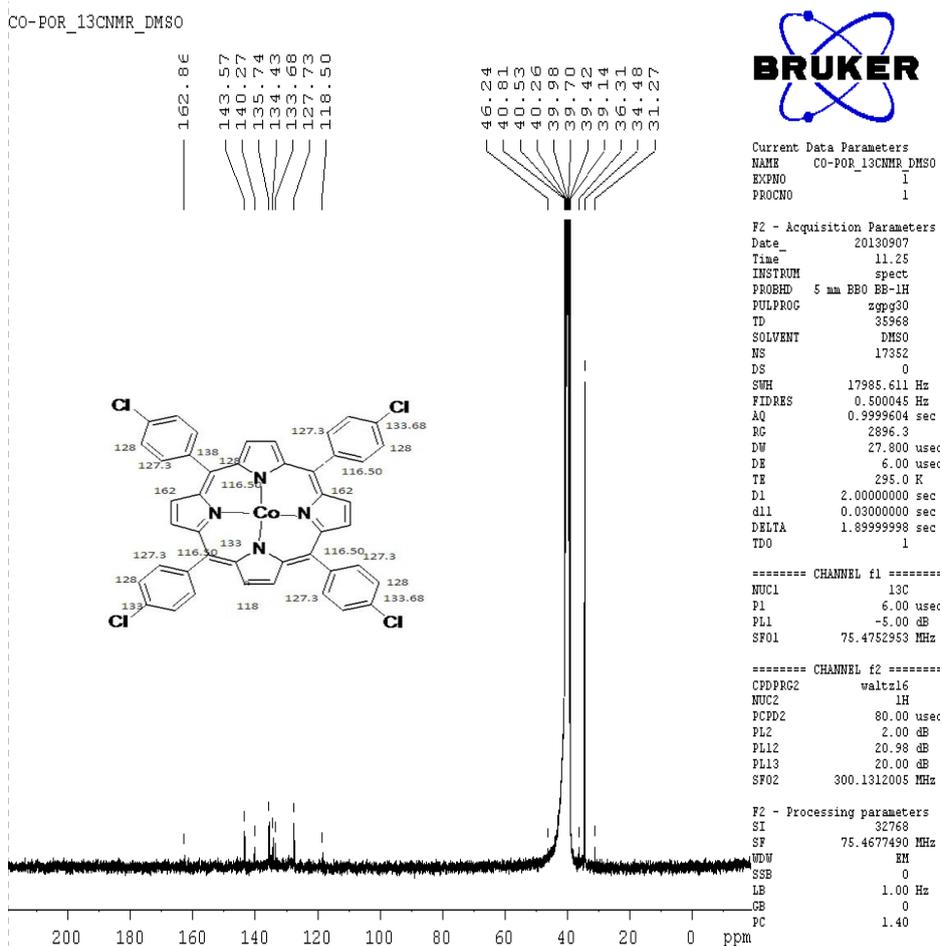
Figure 6. C13 NMR OF TCPPCo.

$$G_{\text{out of plane}} = 3A1U + 6A2U \text{ (IR)} + 4B2U + 5B1U + 8E_g \text{ (R)}$$

The 8 E_g modes are Raman active and 6 $A2_g$ modes are infrared active. Raman spectra is based on statistics analysis, the in plane modes are dominant than out of plane modes. There is also number of phenyl vibrations as compared to central TCPP core. In order to consider phenyl group chlorobenzene has been set as a model. The TCPP ligand has four phenyl groups which is bounded to meso carbon atom of porphyrin core. So there are four asymmetry adaptation combinations in TCPP. These interactions are small so obtained splitting among four phenyl rings are small (5-10 cm^{-1}). So it is of C_{2V} (Point group of chlorophenyl), four different symmetry blocks are found. There are 169 normal modes, 44% are Raman active and 27% are IR active. Interaction (C_1) intense sort and weak Q band can be observed. The band is observed on the higher side of Q. This band Q_V is due to vibronic mixing between sort and Q band. Both excitation vibrations are of E_U Symmetry. The Q and Q_V spectrum confirms the formation of complexes. There are three effects which can affect the D_{4h}. The first effect is phenyl ring, coupling between core and strong phenyl ring vibration. The second effect is different mixed modes. The third effect is symmetry lowering beyond C_{4V} is the degenerate E_U vibration split in IR spectra [15].

4. Conclusions
Raman spectroscopy and infra-red spectroscopy successfully explained the structure and properties of tetraphenyl porphyrin metal complexes.

5. References

1. Mantsch, H. H. and Chapman, D. (Eds), Infrared Spectroscopy of Biomolecules, Wiley, New York, 1996.

2. Clark, R. J. H. and Hester, R. E., Biomedical Applications of Spectroscopy, Wiley, Chichester, UK, 1996.

3. Kalasinsky, V. F., Appl. Spectrosc. Rev., 31, 193–249 (1996).

4. Naumann, D., Appl. Spectrosc. Rev., 36, 239–298 (2001).

5. Fabian, H., 'Fourier Transform Infrared Spectroscopy in Peptide and Protein Analysis', in Encyclopedia of Analytical Chemistry, Vol. 7, Meyers, R. A. (Ed.), Wiley, Chichester, UK, 2000, pp. 5779–5803.

6. Barth, A., Prog. Biophys. Mol. Biol., 74, 141–173 (2000).

7. Byler, D. M. and Susi H., Biopolymers, 25, 469–487 (1986).

8. Shaw, R. A. and Mantsch H. H., J. Mol. Struct., 480–481, 1–13 (1999).

9. Wentrup-Byrne, E., Rintoul, L., Smith, J. L. and Fredericks, P. M., Appl. Spectrosc., 49, 1028– 1036 (1995).

10. Estepa, L. and Daudon, M., Biospectroscopy, 3, 347–369 (1997).

11. Rothemund, P., Formation of Porphyrins from Pyrrole and Aldehydes. Journal of the American Chemical Society (1935).

12. Adler, A. D.; Longo, F. R.; Finarelli, J. D.; Goldmacher, J.; Assour, J.; Korsakoff, L., A simplified synthesis for meso-tetraphenylporphine. The Journal of Organic Chemistry (1967).

13. McIntosh, L. M. and Jackson, M., 'ex vivo Vibrational Spectroscopy Imaging', in Handbook of Vibrational Spectroscopy, Vol. 5, Chalmers, J. M. and Griffiths, P. R. (Eds), Wiley, Chichester, UK, (2002).

14 Alam, M. K., 'Non-Invasive Diagnosis by Near-Infrared Spectroscopy', in Handbook of Vibrational Spectroscopy, Vol. 5, Chalmers, J. M. and Griffiths, P. R. (Eds), Wiley, Chichester, UK, (2002).

15 Gremlich, H.-U. and Yan, B., Infrared and Raman Spectroscopy of Biological Materials, Marcel Dekker, New York, (2000).